various degrees. The CK meteorites may be metamorphosed carbonaceous chondrite material, but if so, the metamorphism was of the closed-system variety. Patterns of labile trace elements in three CK chondrites resemble those of 39 other carbonaceous chondrites (*14*) and contrast sharply with those of the three unusual CI-CM chondrites (*5*) and heated Murchison (*7*), determined in an open system. With regard to trace elements and spectral reflectances, no CK metamorphism was identical to that experienced by the large C, G, B, and F asteroids whose spectra have been measured, which suggests that the process of metamorphism varied among the asteroids.

The difference between most carbonaceous chondrites and the C, G, B, and F asteroid surface materials may lie in the fact that all the observed asteroids are large [10 to 1000 km in diameter (*6*, *9*)], with a possibly greater opportunity to have been thermally metamorphosed. Friable, unmetamorphosed surface materials similar to most carbonaceous chondrites could have been abraded away by subsequent impact processing, forming smaller asteroids and fragments. The carbonaceous chondrites we now have may derive from a restricted, unrepresentative number of small relatives of the C, G, B, and F asteroids, located at dynamically favorable positions. There has been a similar problem in relating the common S asteroids to the ordinary chondrites, and it has been suggested that the ordinary chondrites are also derived predominantly from small unobserved asteroids (*13*).

Infrared reflectance spectra of CI and CM chondrites usually show strong absorption bands around 3 μm because of hydrated silicates, and the unusual, naturally heated CI-CM chondrites B7904, Y82162, and Y86720 still show a weak absorption band near 2.9 μm (*15*). Similar absorption bands were also observed for many C, G, B, and F asteroids (*16*). Thermal metamorphism of the unusual CI-CM chondrites and these asteroids should have been heterogeneous, preserving some relatively unheated materials. It is also possible that the asteroids were originally formed of anhydrous silicates and water ice and that those silicates subsequently underwent different degrees of aqueous alteration. If the observed 3.1-μm band of 1 Ceres (*16*) is attributable to water ice, Ceres may not have undergone any extensive thermal metamorphism.

REFERENCES AND NOTES

1. Classifications are based on those of D. J. Tholen [in *Asteroids II*, R. P. Binzel, T. Gehrels, M. S. Matthews, Eds. (Univ. of Arizona Press, Tucson, 1989), pp. 1139–1150].
2. T. V. Johnson and F. P. Fanale, *J. Geophys. Res.* **78**, 8507 (1973); F. Vilas and M. J. Gaffey, *Science* **246**, 790 (1989).
3. M. J. Gaffey, *J. Geophys. Res.* **81**, 905 (1976).
4. C. R. Chapman and M. J. Gaffey, in *Asteroids*, T. Gehrels, Ed. (Univ. of Arizona Press, 1979), pp. 1064–1089; J. F. Bell, P. D. Owensby, B. R. Hawke, M. J. Gaffey, *Lunar Planet. Sci.* **19**, 57 (1988).
5. K. Tomeoka, H. Kojima, K. Yanai, *Proc. NIPR Symp. Antarct. Meteorites* **2**, 36 (1989); *ibid.*, p. 55; K. Tomeoka, *ibid.* **3**, 40 (1990); J. Akai, *ibid.*, p. 55; R. L. Paul and M. E. Lipschutz, *ibid.*, p. 80; Y. Ikeda, *ibid.* **5**, 49 (1992).
6. E. F. Tedesco, in *Asteroids II*, R. P. Binzel, T. Gehrels, M. S. Matthews, Eds. (Univ. of Arizona Press, Tucson, 1989), pp. 1090–1138.
7. S. D. Matza and M. E. Lipschutz, *Proc. Lunar Planet. Sci. Conf.* **8**, 161 (1977).
8. M. E. Zolensky and H. Y. McSween, Jr., in *Meteorites and the Early Solar System*, J. F. Kerridge and M. S. Matthews, Eds. (Univ. of Arizona Press, Tucson, 1988), pp. 114–143; M. E. Zolensky, R. Barrett, L. Browning, *Geochim. Cosmochim. Acta*, in press.
9. B. Zellner, D. J. Tholen, E. F. Tedesco, *Icarus* **61**, 355 (1985).
10. T. V. V. King, thesis, University of Hawaii (1986).
11. J. Gradie and J. Veverka, *Proc. Lunar Planet. Sci. B* **12**, 1769 (1981).
12. D. J. Tholen, thesis, University of Arizona (1984).
13. J. F. Bell, D. R. Davis, W. K. Hartmann, M. J. Gaffey, in *Asteroids II*, R. P. Binzel, T. Gehrels, M. S. Matthews, Eds. (Univ. of Arizona Press, Tucson, 1989), pp. 921–945.
14. X. Xiao and M. E. Lipschutz, *J. Geophys. Res.* **97**, 10199 (1992).
15. M. Miyamoto, *Proc. NIPR Symp. Antarct. Meteorites* **5**, 155 (1992).
16. M. A. Feierberg, L. A. Lebofsky, D. J. Tholen, *Icarus* **63**, 183 (1985); T. D. Jones, L. A. Lebofsky, J. S. Lewis, M. S. Marley, *ibid.* **88**, 172 (1990).

17. We thank J. F. Bell for the 52-color asteroid reflectance spectra; M. Miyamoto and H. Y. McSween, Jr., for helpful suggestions; F. Vilas and M. J. Gaffey for the review of the manuscript; the National Institute of Polar Research and the Meteorite Working Group for the loan of antarctic meteorites; Brown University, where reflectance spectra of meteorite powders were measured at RELAB, a multiuser facility operated under National Aeronautics and Space Administration (NASA) grant NAGW-748; and S. Pratt for assistance with the measurements. Supported by NASA grants NAG 9-48 (M.E.L.) and NAGW-28 (C.M.P.) and by the NASA Origins of Solar Systems Program (M.E.Z.). This work was done while T.H. held a National Research Council–NASA/Johnson Space Center Research Associateship.

29 March 1993; accepted 1 July 1993

Surface Tension Measurements of Surface Freezing in Liquid Normal Alkanes

X. Z. Wu, B. M. Ocko, E. B. Sirota, S. K. Sinha, M. Deutsch, B. H. Cao, M. W. Kim

Surface tension measurements reveal surface freezing in liquid *n*-alkanes. A solid monolayer of molecules is found to exist up to 3°C above the bulk freezing point. This surface phase exists only for carbon numbers $14 < n \leq 50$. The measured carbon number and temperature dependence of the surface tension is interpreted within a simple thermodynamical model based on known bulk latent heat data and surface energy considerations. The vanishing of the surface phase for $n \leq 14$ is a possible transition from surface freezing to surface melting behavior.

The role of the free surface in the nucleation of bulk melting or freezing is a subject of much current theoretical (*1–3*) and experimental (*4–10*) interest. As two-dimensional critical temperatures are in general lower than their three-dimensional counterparts, surface melting, where an equilibrium layer of the melt wets the surface of a solid at temperatures below its bulk freezing point T_f, is typical of virtually all solids studied (*1*). It has been observed in a variety of different systems, such as metals (*4*), semiconductors (*5*), inert gas films (*6*), ice (*7*), and most recently, molecular crystals (*8*). By contrast, the opposite phenomenon of surface freezing, where an ordered layer forms at the surface of an isotropic liquid above its bulk freezing point, was observed only in liquid crystals (*9*) and alkanes (*10*). The freezing phenomena in these systems appear to be related: The alkane hydrocarbon chain is a basic component of liquid crystals; however, the liquid crystal surface layers exhibit only liquid-like order (*9*), whereas the order in the alkane surface layer is crystalline (*10*). Surface freezing and melting effects are classified as wetting phenomena, where the system's free energy is lowered when the bulk's surface is wetted by the different surface phase. The thickness of the surface layer at a given temperature is determined by the balance between surface and bulk energies. As the balance is temperature-dependent in general, a system may exhibit either complete wetting, for which the surface layer thickness diverges upon approaching T_f, or partial wetting, for which it remains finite at T_f. To our knowledge, no system exhibiting a transition from surface freezing to melting behavior has been reported.

X. Z. Wu, E. B. Sirota, S. K. Sinha, B. H. Cao, M. W. Kim, Corporate Research Science Laboratory, Exxon Research and Engineering Co., Annandale, NJ 08801.
B. M. Ocko, Physics Department, Brookhaven National Laboratory, Upton, NY 11973.
M. Deutsch, Physics Department, Bar Ilan University, Ramat Gan 52900, Israel.

Normal alkanes, which are linear hydrocarbon chains, CH_3-$(CH_2)_{n-2}$-CH_3 (denoted C_n), are among the most basic constituents of organic molecules. They form part of lipids, surfactants, liquid crystals, and polymers (*11*). Hence, they are immensely important for both basic science and industrial applications. The surface structure of these materials is the subject of much current theoretical (*12*) and experimental (*10, 13, 14*) research. We report here surface tension measurements on liquid *n*-alkanes showing the existence of a surface ordered layer at temperatures up to $\Delta T = 3$°C above the bulk freezing temperature. Compared with the bulk values, the surface entropy variations calculated from the surface tension data reveal that the structure of the surface layer is similar to the bulk R_{II} rotator phase (*15*), where the chains are vertically aligned and hexagonally packed with long-range positional order, consistent with our x-ray measurement (*10*). The wetting of the bulk alkane liquid by the rotator phase is found here to be strongly incomplete, as only a single solid monolayer is formed down to T_f. We measured the (n, ΔT) phase diagram and found the monolayer to exist only for carbon numbers in the range of $14 < n \leq 50$. The vanishing of the layer for $n \leq 14$ represents a crossover from surface freezing to the common surface melting behavior. A simple thermodynamical model based on surface energy considerations accounts well for the observed trends and the phase diagram. Surface tension measurements similar to ours for a range of $15 \leq n \leq 18$ were very recently reported by Earnshaw and Hughes (*14*); however, the crystalline monolayer nature of the surface phase and the full phase diagram were not elucidated in that study.

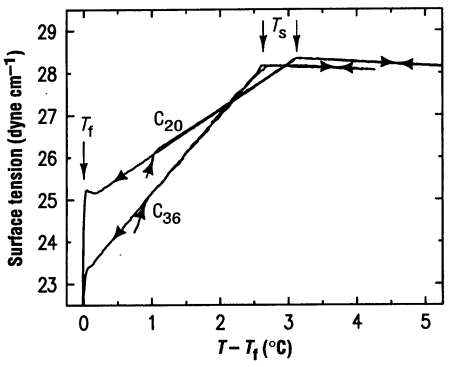

Fig. 1. The surface tensions γ of C_{20} and C_{36} measured in a cooling and heating cycle (arrows denote temperature-scan directions). The curves are shifted so that their freezing point T_f is at the origin. Note the sharp cusp at T_s (indicating the formation of the monolayer), the equal slopes above it, and the different slopes below.

The surface tension was measured with a thin, roughened Platinum Wilhelmy plate (*16*), 2.5 cm wide, attached to an electronic balance. The samples were contained in a temperature-regulated cell, the cover of which had a small hole to pass the wire connecting to the plate. Because the vapor pressure of the alkanes studied is small near melting, the closure of the cell is unimportant, as indicated by the agreement with the x-ray results obtained in a closed cell. The temperature was controlled to ≤0.005°C with a cross-cell gradient ≤0.010°C. The gradient was sufficiently small to have a negligible effect on the experimental results. A data point was measured every 30 s while the temperature was varied at ≤0.0003°C s^{-1} to ensure ample thermal equilibration. Slowing the scan rate and changing the scan direction did not alter the results. All samples (99% pure commercial products from Sigma, Aldrich, or Fluka) were used as received (*17*).

Measurements of the surface tension γ during a complete cooling-heating cycle for C_{20} and C_{36} are shown in Fig. 1. The clear cusp marks T_s, the onset of surface freezing. At this temperature, the slope of γ changes abruptly from a small negative value for $T > T_s$, typical of simple liquids, to a large positive value for $T < T_s$. This change is a clear indication of the formation of an ordered surface layer on top of the bulk liquid, as discussed for the related surface effects observed in sodium dodecyl sulfate–water lyotropics (*18*). Similar arguments were used for the more remotely related surface layering effects in liquid metals (*19*). Because γ is equal to the excess free energy per unit area of the surface over the bulk (*16*), it can be written as:

$$\gamma = \epsilon' - T(S' - S) \quad (1)$$

where ϵ' is the excess surface energy per unit area and S' and S are the entropy densities in the surface layer and the bulk liquid, respectively. For the normal liquid surface at $T > T_s$, the surface molecules are less constrained than those in the bulk, and thus S' is slightly larger than S, yielding $d\gamma/dT = -(S' - S) < 0$. As the surface freezes at $T = T_s$, the molecules at the surface become more constrained than those in the bulk so that $S' << S$, leading to $d\gamma/dT = -(S' - S) > 0$. The abrupt change of slope seen in Fig. 1 suggests a first-order transition, with little hysteresis and no pretransitional effects. The absence of any further slope changes implies that no further layering occurs down to bulk freezing (*10*).

The slope for $T > T_s$ is relatively small and constant with n, whereas the slope for $T < T_s$ is larger and changes significantly with n (Fig. 1). For all alkanes measured, we obtained $(d\gamma/dT)_{T>T_s} = -0.09 \pm 0.01$ dyne cm^{-1} °C^{-1}, consistent with the literature values (*11, 20*). By contrast, the slope for $T < T_s$ increases with n. Denoting the slope difference above and below T_s by

$$\Delta(d\gamma/dT) = (d\gamma/dT)_{T<T_s} - (d\gamma/dT)_{T>T_s} \quad (2)$$

we find experimentally a linear carbon number dependence given by $\Delta(d\gamma/dT) = 0.020 + 0.051n$ erg cm^{-2} °C^{-1}. Noting from Eq. 1 that $\Delta(d\gamma/dT) = \Delta S = -(S'_{T<T_s} - S'_{T>T_s})$, the linear n dependence can be reproduced by ascribing the relevant entropies to chain conformation statistics. Successive C-C links in a chain can have two gauche and one trans conformations, the latter having the lowest energy (*21*). Approximating the chains in the liquid state to be completely flexible so that each bond conformation is of equal probability, the entropy density per chain is $(S'_{T>T_s})_{calc} = k_B \ln 3^{n-3}/A = k_B(n - 3)\ln 3/A$, where k_B is the Boltzmann constant and A is the area per chain. Upon ordering, the conformational degrees of freedom of chains on the surface are greatly reduced, and all bonds can be assumed to be trans. Approximating the solid layer's entropy to be zero, $(S_{T<T_s})_{calc} \approx 0$, and using A = 20 Å^2 per chain [derived from our x-ray measurements (*10*)], we obtain $\Delta(d\gamma/dT)_{calc} = k_B(n - 3)\ln 3/20 = 0.0758(n - 3)$ erg cm^{-2} °C^{-1}. This approximation (Fig. 2A, line) systematically overestimates the experi-

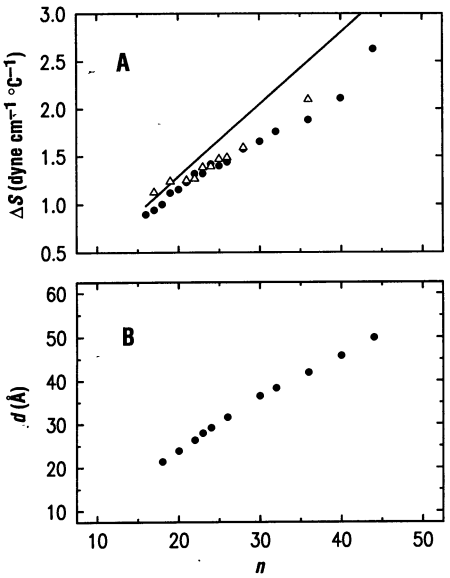

Fig. 2. (**A**) The slope of the surface tension and the entropy differences as a function of carbon number n. The solid circles are the measured slope differences above and below T_s, the line is the theoretical estimation $k_B(n - 3)\ln 3/A$ based on conformation statistics, and the triangles are the estimates based on the measured bulk entropy changes. (**B**) The layer thickness d, as measured directly by x-ray reflectivity, for various n.

mental values (Fig. 2A, circles). Nevertheless, it accounts for the linear n dependence of the slope. More realistically, we can approximate the monolayer-phase entropy density by that of the bulk rotator phase, so that $\Delta(d\gamma/dT)_{calc}$ equals the measured (*11*) entropy change in the bulk liquid-rotator transition. This approximation (Fig. 2A, triangles) is in excellent agreement with our measurements. This excellent agreement validates, therefore, our initial assumptions that the solid monolayer has a structure similar to that of the bulk rotator phase and that the surface phase is only one molecular layer thick. This conclusion is supported strongly by the x-ray reflectivity measurements of the layer thickness d (Fig. 2B). Both the absolute value of d, which correlates closely with the extended molecular length, and its linear n dependence are unambiguous evidence for the existence of a monolayer on the surface. The x-ray measurements of the density and in-plane structure of the monolayer further support the surface tension results (*10*, *22*).

Our γ data at a constant T = 30°C (for examples of T_s > 30°C, values extrapolated from $T > T_s$ were used) are consistent with literature values (Fig. 3), which together can be described by $\gamma_{T=30°C} = \gamma_\infty - \alpha/n^{2/3}$. This relation is based on considerations of the free volume associated with the ends of the chain (*20*, *23*). Not surprisingly, the coefficients γ_∞ = 37.2 dyne cm^{-1} and α = 65.4 dyne cm^{-1} obtained (*22*) are also in good agreement with the literature values (*23*). The surface tension at the onset of the monolayer phase (Fig. 3, circles) is practically constant over the measured range of n, $\gamma_{T_s} \approx c$ with c = 28 dyne cm^{-1}. The n dependence of γ_{T_f} can be understood by noting that the excess free energy of a monolayer at the surface compared with one deep in the bulk solid is a result of the missing interaction with the nonexistent overlayers above the surface. Assuming that the dominant interaction is van der Waals type, the excess free energy varies as $1/d^2$, where $d \sim n$ is the layer spacing (*24*). It is easy to show (*22*) that for this case, the expected n dependence of γ_{T_f} is $\gamma_{T_f} = \gamma'_\infty + \beta/n^2$. This dependence is indeed found in our measurements (Fig. 3, squares), with γ'_∞ = 22.0 dyne cm^{-1} and β = 1200 dyne cm^{-1}.

The (n, ΔT) phase diagram has been derived from our surface tension measurements (Fig. 4). It demonstrates that the new surface phase appears only for $14 < n \leq 50$ and has a maximum range of $\Delta T = T_s - T_f \approx 3$°C. Using free energy considerations and noting that the free energy of bulk liquid equals that of bulk solid at T_f and the free energy of surface liquid equals that of surface solid at T_s, one may calculate (*22*) the temperature range

$$\Delta T = \frac{\gamma_{T_s} - \gamma_{T_f}}{S - S'} \quad (3)$$

Using $(S - S') \sim n$, as done before, and the explicit n dependences found above for γ_{T_f} and γ_{T_s}, we obtain from Eq. 3

$$\Delta T \approx \frac{1}{n}\left(c - \gamma'_\infty - \frac{\beta}{n^2}\right) = \frac{a}{n} - \frac{b}{n^3} \quad (4)$$

where a and b are positive constants (*22*). Equation 4 clearly shows that for small n, ΔT is negative, and hence the surface layer is always disordered at temperatures above T_f. For very large n, the entropy shrinks the ordered surface phase to a small temperature range: $\Delta T \rightarrow 0$ for $n \rightarrow \infty$. Only for intermediate n does an ordered surface phase exist with a significant temperature range. This simple surface energy model accounts for the vanishing of the ordered surface phase for $n \leq 14$. As mentioned before, the transition from positive to negative ΔT is a carbon number–dependent transition from surface freezing to the common surface melting behavior. Fitting the measured data with Eq. 4 (Fig. 4, line) yields a satisfactory agreement. The faster than predicted falloff for $n \geq 44$ is caused by other disordering mechanisms not accounted for in our simple model, which become dominant in this range. These may be internal degrees of freedom such as the proliferation of gauche transformations and the associated loss of average linearity of the molecule.

Further measurements on other compounds (*22*) indicate that the surface behavior found here may be fundamental to many linear chain molecules. One may even wonder whether the surface freezing behavior found in liquid crystals (*9*, *25*) or even some of their bulk liquid crystalline properties, which are usually thought to be dominated by the rigid molecular cores, are in fact attributable to the long chain tails of these molecules. Measurements on similar compounds, as well as a more fundamental theoretical treatment than the simple model presented here, will be most helpful in the elucidation of these questions, shedding further light on the microscopic-level origins of the results presented here.

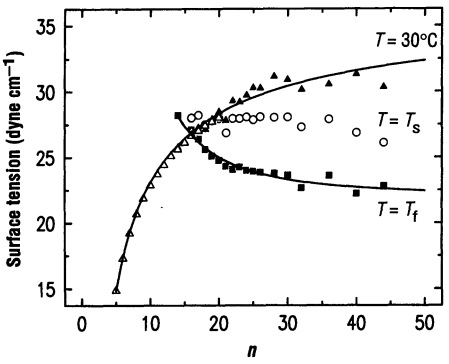

Fig. 3. The surface tension γ measured at the bulk freezing temperature T_f (squares), the surface phase transition temperature T_s (circles), and T = 30°C (solid triangles), compared with the literature data at T = 30°C (open triangles). The lines are fits of the theoretical expressions discussed in the text.

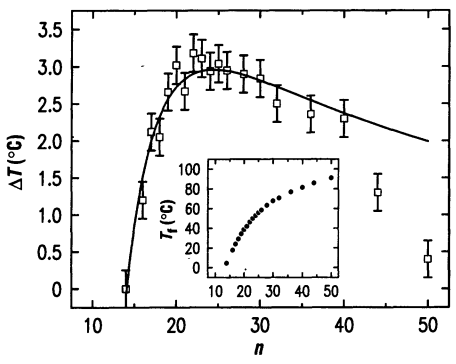

Fig. 4. The measured phase diagram of the monolayer phase (squares) and the fit (line) of the theoretical expression Eq. 4. Note the good agreement for $n \leq 40$ and the faster than predicted falloff for $n > 40$, which is caused by the increasing importance of additional disordering mechanisms. (**Inset**) The bulk freezing temperatures as a function of carbon number.

REFERENCES AND NOTES

1. J. G. Dash, *Contemp. Phys.* **30**, 89 (1989).
2. R. Lipowsky, *J. Appl. Phys.* **55**, 2485 (1984), and references therein.
3. G. An and M. Schick, *Phys. Rev. B* **37**, 7534 (1988).
4. J. W. M. Frenken and J. F. van der Veen, *Phys. Rev. Lett.* **54**, 134 (1985); H. Dosch, T. Höfer, J. Peisl, R. L. Johnson, *Europhys. Lett.* **15**, 527 (1991).
5. A. W. Denier van der Gon, J. M. Gay, J. W. M. Frenken, J. F. van der Veen, *Surf. Sci.* **241**, 335 (1991).
6. D. M. Zhu and J. G. Dash, *Phys. Rev. Lett.* **57**, 2959 (1986); *ibid.* **60**, 432 (1988).
7. M. Elbaum and M. Schick, *ibid.* **66**, 1713 (1991).
8. S. Chandavarkar, R. M. Geertman, W. H. de Jeu, *ibid.* **69**, 2384 (1992).
9. B. M. Ocko, A. Braslau, P. S. Pershan, J. Als-Nielsen, M. Deutsch, *ibid.* **57**, 94 (1986).
10. X. Z. Wu, E. B. Sirota, S. K. Sinha, B. M. Ocko, M. Deutsch, *ibid.* **70**, 958 (1993).
11. D. M. Small, *The Physical Chemistry of Lipids* (Plenum, New York, 1986).
12. T. K. Xia, J. Ouyang, M. W. Ribarsky, U. Landman, *Phys. Rev. Lett.* **69**, 1967 (1992); J. G. Harris, *J. Phys. Chem.* **96**, 5077 (1992).
13. L. Askadskaya and J. P. Rabe, *Phys. Rev. Lett.* **69**, 1395 (1992); J. P. Rabe and S. Buchholz, *Science* **253**, 424 (1991).
14. J. C. Earnshaw and C. J. Hughes, *Phys. Rev. A* **46**, R4494 (1992).
15. The R_{II} rotator phase appears between the low-temperature crystal phase and the high-temperature liquid phase, see (*11*); E. B. Sirota, H. E. King, Jr., D. M. Singer, H. Shao, *J. Chem. Phys.* **98**, 5809 (1993).
16. G. L. Gaines, *Insoluble Monolayers at the Liquid Gas Interface* (Wiley, New York, 1966).
17. Our results were completely reproducible for

samples from different sources and upon cycling repeatedly through the melting point. These are strong indications against ascribing the layer to surface-active contaminants (*10, 14*). The x-ray measurements (Fig. 2B) (*10*), which show a sharply defined layer of uniform thickness closely correlated with *n*, virtually exclude the possibility of contaminants of lengths significantly different from *n*.

18. B. Berge, L. Faucheux, K. Schwab, A. Libchaber, *Nature* **350**, 322 (1991).
19. C. A. Croxton, *Statistical Mechanics of the Liquid Surface* (Wiley, New York, 1980). With the lack of x-ray or neutron measurements, no clear structural evidence is available for the proposed layering. Furthermore, the in-plane order in the postulated layers, if any, is not known. Reference to these effects in liquid metals as surface freezing is therefore premature at present.
20. J. Timmermans, *Physico-Chemical Constants of Pure Organic Compounds* (Elsevier, New York, 1965); C. I. Poser and I. C. Sanchez, *J. Colloid Interface Sci.* **69**, 539 (1979).
21. P.-G. de Gennes, *Scaling Concepts in Polymer Physics* (Cornell Univ. Press, Ithaca, NY, 1979).
22. X. Z. Wu, E. B. Sirota, S. K. Sinha, B. M. Ocko, M. Deutsch, in preparation.
23. D. G. Legrand and G. L. Gains, Jr., *J. Colloid Interface Sci.* **31**, 162 (1969); D. N. Theodorou, *Macromolecules* **22**, 4578 (1989).
24. J. N. Israelachvili, *Intermolecular and Surface Forces* (Academic Press, Orlando, FL, 1985); J. Mahanty and B. W. Ninham, *Dispersion Forces* (Academic Press, New York, 1976).
25. D. E. Moncton, R. Pindak, S. C. Davey, *Phys. Rev. Lett.* **49**, 1865 (1982); E. B. Sirota, P. S. Pershan, S. Amador, L. B. Sorensen, *Phys. Rev. A* **35**, 2283 (1987); B. D. Swanson, H. Straiger, D. J. Tweet, L. B. Sorensen, *Phys. Rev. Lett.* **62**, 909 (1989); R. Holyst, *Phys. Rev. A* **44**, 3692 (1991).
26. Supported by The U.S.–Israel Binational Science Foundation, Jerusalem (M.D.). Brookhaven National Laboratory is supported by the Division of Materials Research, U.S. Department of Energy under contract DE-AC02-76CH00016.

1 April 1993; accepted 22 June 1993

Giant Magnetoresistance at Low Fields in Discontinuous NiFe-Ag Multilayer Thin Films

T. L. Hylton, K. R. Coffey, M. A. Parker, J. K. Howard

A series of sputtered multilayers of $Ni_{80}Fe_{20}$-Ag was prepared to examine the giant magnetoresistance effect before and after annealing. For a wide range of NiFe and Ag thicknesses, no giant magnetoresistance was observed in the unannealed films. After annealing, a large, negative magnetoresistance was observed of order 4 to 6% in applied fields of order 5 to 10 oersteds at room temperature. The appearance of giant magnetoresistance is concurrent with the breakup of the NiFe layers, which is attributable to a magnetostatic interaction that favors local antiparallel alignment of the moments in adjacent layers. These structures may be of significant practical importance as sensors that require large changes in resistance at low fields, such as magnetoresistive heads used in magnetic recording systems.

Since the discovery of giant magnetoresistance (GMR) in Fe-Cr sandwiches (*1, 2*), GMR has been observed in a variety of magnetic-nonmagnetic multilayer (*3, 4*) and granular alloy systems (*5–7*). The smallest values of resistance are observed in these systems when the magnetization of neighboring layers or clusters is aligned by an applied field, and larger values of resistance are observed when neighboring layers are antialigned or neighboring clusters are "randomly" aligned. With the exception of the spin-valve devices (*4*) and related devices (*8, 9*), the fields necessary to achieve magnetic saturation and a significant magnetoresistive effect are generally too large to make these devices promising in low-field sensor applications. For many multilayer systems, the magnitude and sign of the interlayer exchange coupling is a strong function of the nonmagnetic layer thickness (*10*), which can lead to difficulties in the preparation of the weakly antiferromagnetically coupled structures necessary for low-field sensitivity. For alloy systems, the particle size, shape, and temperature dominate the field dependence of the GMR with the result that low-field sensitivity is not possible in realistic alloy systems (*11*).

We prepared discontinuous multilayers by annealing sputtered multilayers of $Ni_{80}Fe_{20}$-Ag. We postulate that this structure minimizes the effects of crystal and shape anisotropy, providing a magnetostatically induced, antiparallel coupling between layers. As these samples exhibit 4 to 6% GMR at room temperature in fields of 5 to 10 Oe, they satisfy two important criteria in the design of magnetoresistive sensors for magnetic recording heads: a magnetoresistance greater than 2% and a sensitivity greater than 0.5% per oersted. Other equally important criteria, such as noise, durability, and manufacturability, may or may not be satisfied and are the subject of ongoing efforts.

The original motivation for this work is our own theoretical (*11*) and experimental work on GMR in granular alloys of Co-Cu and NiFe-Ag (*12*) and granular, evaporated bilayers of Cu-NiFe and Cu-Co (*13*). The large fields (typically 10 kOe in alloys and 1 kOe in bilayers) necessary to achieve significant GMR in these granular alloys can be attributed to three effects: (i) The typical particle sizes in these systems (20 to 40 Å) are so small that thermal fluctuations easily disorient the particles at a nominal 10-Oe applied field, which we define as "low"; (ii) the anisotropy fields induced by departures in shape of only a few percent from perfect spheres can be large compared with 10 Oe; and (iii) crystalline anisotropy fields are expected to be large compared with 10 Oe in all but the softest alloys, such as $Ni_{80}Fe_{20}$.

The second consideration suggests that greater low-field sensitivity can be achieved if the collection of particles can be given a flat, disk-like shape and oriented such that all the particle surfaces are parallel to the applied field. The in-plane anisotropy induced by departures from a perfectly circular perimeter will be much smaller than in the case of similarly misshapen spherical particles. In an effort to achieve such a structure, we prepared annealed multilayers of immiscible magnetic (NiFe) and nonmagnetic materials (Ag). Under appropriate annealing conditions, we expect penetration of the nonmagnetic material at the grain boundaries of the magnetic layer. Although this may or may not result in a collection of flat, island-like magnetic particles, it will certainly promote a multidomain state within the magnetic layers. These discontinuous multilayers should show properties similar to both continuous multilayers and granular alloys. We chose the NiFe-Ag system because we desired a low anisotropy magnetic alloy and an immiscible spacer material.

The multilayers were prepared by S-gun magnetron sputtering in a mixture of 4% H_2 and 96% Ar at a pressure of 3 mtorr with substrates at ambient temperature. Substrates were 1-inch Si wafers with a thermally grown oxide surface 700 Å thick. A typical sample with n layers of NiFe of thickness x and Ag of thickness y is given by Ta(100 Å)-Ag(y/2)-[NiFe(x)-Ag(y)]$_{n-1}$-NiFe(x)-Ag(y/2)-Ta(40 Å)-SiO_2(700 Å)-Si. A magnetic field of approximately 150 Oe, applied during deposition, resulted in a weak uniaxial anisotropy field of 2 to 3 Oe with significant dispersion. After deposition, the samples were broken into strips of about 8 mm by 1.5 mm and were annealed at atmospheric pressure in a mixture of 5% H_2 and 95% Ar in a rapid thermal processing oven at a variety of temperatures for 10 min. Magnetoresistance measurements were performed with a four-point, in-line geometry of the contacts with the magnetic field applied parallel to the plane of the sample and either perpendicular or parallel to the current direction. Magnetization measurements

IBM ADSTAR, San Jose, CA 95193.